

Buscar correo



Activo



← → ⌂ ⌃ ⌄ ⌅ ⌆ ⌇ ⌈ ⌉ ⌊ ⌋

1 de 2.205 ⌈ ⌉

Paper 143 summary

Externo

Recibidos x



Microsoft CMT <noreply@msr-cmt.org>

para mí ▾

23:46 (hace 1 minuto)



Hello.

Here is submission summary.

Track Name: ISGTA2025

Paper ID: 143

Paper Title: DEVELOPMENT AND ANALYSIS OF THE DEEPKRIGING HYBRID MODEL FOR THE SPATIAL ESTIMATION OF AGRICULTURAL DROUGHTS IN PUNO

Abstract:

Agricultural droughts in the Peruvian Altiplano pose a critical threat to food security, affecting the production of quinoa and native potatoes that sustain over 800,000 rural inhabitants. This study develops and implements a hybrid model of Spatial Deep Convolutional Neural Network (SDCNN) with geostatistical integration through Deep Kriging, aimed at the spatial estimation of the Standardized Precipitation Index (SPI-6) from satellite images (Sentinel-2, MODIS) and climatic variables (ERA5). The architecture combines multiresolution convolutional branches based on radial basis functions with dense layers that integrate climatic covariates, while the Monte Carlo Dropout scheme enables the quantification of epistemic and aleatoric uncertainty.

The model achieved robust performance on the test set ($R^2=0.8337$, RMSE = 0.2321, MAE = 0.1873, NSE = 0.8337), surpassing reference methods such as ordinary Kriging and linear regression. The uncertainty decomposition showed average values of indicating that nearly 89% of the total error comes from natural climatic variability. The system enables early drought detection with up to two months of anticipation and generates spatially explicit risk maps that identify optimal zones for quinoa cultivation in the central Altiplano. These results demonstrate the potential of the SDCNN-Deep Kriging approach as an operational tool for proactive management of agroclimatic risks in highly vulnerable Andean regions.

Created on: Mon, 20 Oct 2025 04:45:20 GMT

Last Modified: Mon, 20 Oct 2025 04:45:20 GMT

DEVELOPMENT AND ANALYSIS OF THE DEEPKRIGING HYBRID MODEL FOR THE SPATIAL ESTIMATION OF AGRICULTURAL DROUGHTS IN PUNO

Wladimir Aldo Carlosviza Amanqui¹

Universidad Nacional del Altiplano, Puno, Perú
wcarlosviza@est.unap.edu.pe

Abstract. Agricultural droughts in the Peruvian Altiplano pose a critical threat to food security, affecting the production of quinoa and native potatoes that sustain over 800,000 rural inhabitants. This study develops and implements a hybrid model of Spatial Deep Convolutional Neural Network (SDCNN) with geostatistical integration through *Deep Kriging*, aimed at the spatial estimation of the Standardized Precipitation Index (SPI-6) from satellite images (Sentinel-2, MODIS) and climatic variables (ERA5). The architecture combines multiresolution convolutional branches based on radial basis functions with dense layers that integrate climatic covariates, while the *Monte Carlo Dropout* scheme enables the quantification of epistemic and aleatoric uncertainty.

The model achieved robust performance on the test set ($R^2 = 0.8337$), $RMSE = 0.2321$, $MAE = 0.1873$, $NSE = 0.8337$), surpassing reference methods such as ordinary Kriging and linear regression.

Keywords: agricultural drought, Deep Kriging, convolutional neural networks, SPI-6, uncertainty, Peruvian Altiplano

1 Introduction

Drought is recognized as a common meteorological phenomenon that exerts a significant impact on both natural ecosystems and human activities [2]. The lack of precipitation is the most common initial factor; however, drought manifests in different forms according to its mechanism and its consequences on the environment, classified into meteorological, hydrological, agricultural, and socioeconomic drought [3]. In the Puno region, located in the southeastern Altiplano of Peru (approximately between $13^{\circ}00\text{--}17^{\circ}17\text{ S}$ and $68^{\circ}48\text{--}71^{\circ}08\text{ W}$), the regional economy is primarily supported by rainfed agriculture and South American camelid livestock farming. These activities constitute the fundamental pillars of the sustenance of the rural population, which depends heavily on a seasonal rainfall regime characterized by high variability and unpredictability [4,5,6,7]. SENAMHI reported that, according to the Standardized Precipitation Index (SPI), the southern highlands of Peru, especially Cusco and Puno,

recorded moderate to extreme drought conditions between January and December, evidencing its persistence in the Altiplano [8]. Traditional drought monitoring indices, such as the SPI and PDSI, have been widely used but present relevant shortcomings: the PDSI is mainly limited to the agricultural scope and does not clearly distinguish between meteorological, hydrological, and socioeconomic drought. For its part, the SPI only considers precipitation, leaving aside variables such as evaporation that are critical under climate change conditions [28]. Additionally, many traditional drought indices do not fully integrate information from optical, radar, and thermal satellite sensors, limiting their ability to leverage multimodal data and improve agricultural prediction accuracy [33,32]. These cases demonstrate the need for accurate and timely drought forecasts. Deep learning has positioned itself as an essential tool in artificial intelligence, capable of extracting complex spatio-temporal patterns in geospatial data and improving environmental modeling [13]. In particular, convolutional neural networks (CNNs) have transformed the processing of satellite images by learning hierarchical representations directly from raw data [14]. To overcome this limitation, the *DeepKriging* approach combines the representational capacity of deep learning with the geostatistical robustness of Kriging. This model feeds a set of spatial basis functions and coordinates into a deep neural network, enabling the modeling of complex nonlinear spatial functions and predicting phenomena in highly non-stationary environments [40]. The main objective of this study is to develop and analyze a hybrid *DeepKriging* model for the spatial estimation of agricultural droughts in Puno, quantifying predictive uncertainty and evaluating its applicability in generating recommendations for quinoa and native potato cultivation. Specifically, it seeks: (1) to implement an automated system for extraction and preprocessing of multi-source satellite data (Sentinel-2, MODIS, CHIRPS, and SMAP) using Google Earth Engine; (2) to develop a hybrid *Deep Kriging* architecture (SDCNN) that combines multi-scale convolutional networks with explicit modeling of spatial dependence for SPI-6 prediction; (3) to quantify epistemic and aleatoric uncertainty using Monte Carlo Dropout, generating predictive reliability spatial surfaces.

2 Materials and Methods

2.1 Study Area

The Puno region covers approximately 71,999 km² in the southeastern Peruvian Altiplano, being one of the highest inhabited areas in the world (3,826 m a.s.l.) [18]. In this high-altitude zone, the average annual temperature is around 8–10 °C, with diurnal amplitudes that can exceed 15 °C during winter [16,17]. The rainy season is mostly concentrated between December and March, while the months from May to October experience a marked decrease in precipitation, reinforcing the semi-arid condition characteristic of the altiplano [19].

2.2 Data Sources

The study integrated optical, thermal, and microwave satellite information along with climatic records for the Puno region (2020–2024), processed in *Google Earth Engine* (GEE). Multispectral Sentinel-2A/B images (COPERNICUS/S2_SR collection) were used with a spatial resolution of 10–20 m and a 5-day revisit [20]. From them, three key indices were calculated: the NDVI, which estimates vegetation vigor; the VCI, which assesses relative stress through temporal variation of NDVI; and the NBR, sensitive to canopy moisture and water stress [29,32]. The images were atmospherically corrected and QA60 cloud masks and monthly median composites were applied [20]. Land Surface Temperature (LST) was obtained from the MOD11A1 product (Terra satellite), with 1 km resolution and daily frequency, subsequently aggregated to monthly values and resampled to 10 m for spatial compatibility with Sentinel-2 [32]. Precipitation came from the CHIRPS product, which combines infrared satellite data with in situ observations. Its resolution is 5.5 km daily, aggregated monthly for regional analysis [23]. Surface soil moisture (0–5 cm) was obtained from the SMAP satellite (NASA.USDA/HSL/SMAP10KM_soil_moisture collection), resampled to 10 m. This product combines active radar and passive radiometer measurements, providing key information on edaphic water availability [24].

Standardized Precipitation Index (SPI) The SPI was derived from monthly CHIRPS data on 1, 3, 6, and 12-month scales:

$$\text{SPI} = \frac{P - \mu}{\sigma} \quad (1)$$

where P is the accumulated precipitation, μ the historical mean (1991–2020), and σ the standard deviation [27]. A gamma distribution was used for prior fitting, selecting the SPI-6 for its sensitivity to medium-term agricultural droughts that affect crops such as quinoa and native potatoes [29].

Spatial Sampling 473 sampling points were defined using stratified random design over 71,999 km², covering altitudinal gradients (3,800–5,200 m) and main agroclimatic zones, balancing spatial coverage and computational feasibility [20].

2.3 Target Variable: Standardized Precipitation Index (SPI)

The Standardized Precipitation Index (SPI) was calculated following the classical methodology of [27], defined as:

$$\text{SPI} = \frac{P - \mu}{\sigma} \quad (2)$$

where P is the accumulated precipitation, μ the historical mean (1981–2010), and σ the standard deviation. Previously, the accumulated precipitation was fitted to a two-parameter gamma distribution, estimated by maximum likelihood, ensuring a standard normal distribution $N(0, 1)$ after standardization.

2.4 SDCNN Architecture with Deep Kriging

The proposed hybrid model combines convolutional networks with geostatistics, extending the DeepKriging framework of [40]. Spatial basis functions were defined using fixed-rank Kriging [41] at three resolution levels [42]:

$$\phi(\mathbf{s}, \mathbf{c}_j) = \exp\left(-\frac{\|\mathbf{s} - \mathbf{c}_j\|^2}{2\theta^2}\right) \quad (3)$$

Each level was processed by a parallel convolutional layer with 2×2 filters, whose outputs were vectorized and propagated through dense layers with ReLU activation. Climatic variables (precipitation, temperature, NDVI, VCI, NBR, LST, moisture, and normalized coordinates) were processed in a dense branch with Dropout ($p = 0.3$) and Batch Normalization [34].

The final fusion integrated all representations into a vector \mathbf{H}_i , incorporating a differentiable Kriging layer that models non-stationary spatial dependencies [37]:

$$d_{ij} = \|\mathbf{s}_i - \mathbf{s}_j\|_2 \quad (4)$$

$$O_i = \mathbf{W}'_{\text{out}} \mathbf{H}_i + c_{\text{out}} \quad (5)$$

where O_i is the final SPI-6 prediction.

2.5 Uncertainty Quantification

Uncertainty was estimated using *Monte Carlo Dropout* [43] with 50 stochastic iterations:

$$\hat{y}_{\text{mean}} = \frac{1}{50} \sum_{t=1}^{50} \hat{y}_t, \quad \sigma_{\text{epi}}^2 = \frac{1}{50} \sum_{t=1}^{50} (\hat{y}_t - \hat{y}_{\text{mean}})^2 \quad (6)$$

and the total uncertainty:

$$\sigma_{\text{total}}^2 = \sigma_{\text{epi}}^2 + \sigma_{\text{ale}}^2 \quad (7)$$

allowing differentiation between epistemic uncertainty (model) and aleatoric uncertainty (data) [44].

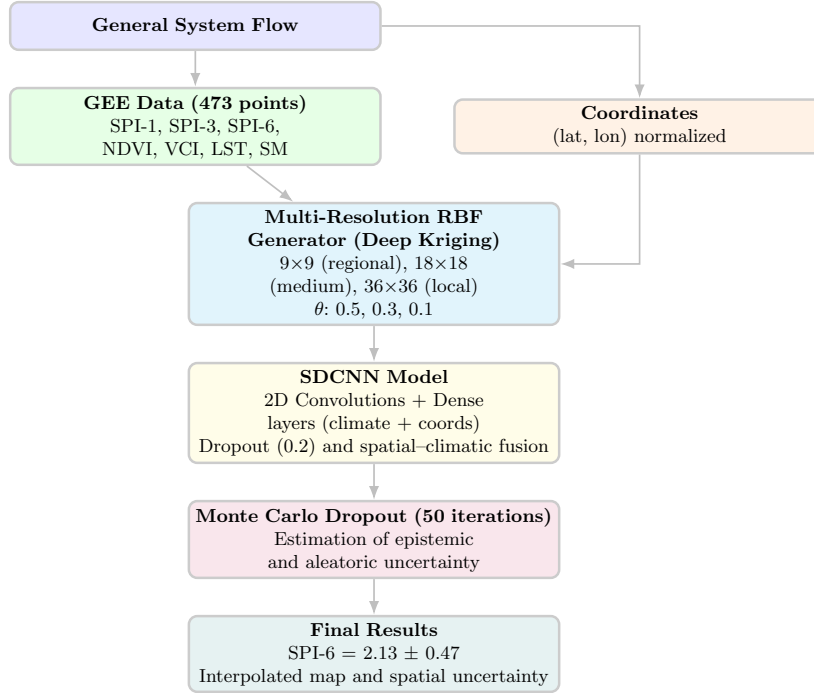


Fig. 1. Methodological flow of the hybrid SDCNN–Deep Kriging system for drought prediction and uncertainty.

3 Results

3.1 SDCNN Predictive Performance

The SDCNN model reached convergence after 26 epochs when Early Stopping detected 15 consecutive epochs without improvement in validation loss. Training loss evolution: monotonic decrease from 0.245 (initial epoch) to 0.0041 (final epoch). Validation loss: decrease from 0.198 stabilizing at 0.0065. Small training-validation gap of 0.0024 confirming low overfitting and good generalization.

Table 1. Performance Metrics

Model	R ²	RMSE	MAE	NSE
SDCNN (proposed)	0.8337	0.2321	0.1873	0.8337

The performance metrics on the test set (Table 1) evidence the solid predictive capacity of the proposed model. The coefficient of determination ($R^2 =$

0.8337) indicates that the model explains approximately 83.37 % of the spatio-temporal variability of the SPI.

The root mean square error (RMSE = 0.2321) represents about 23 % of the observed standard deviation of the SPI ($\sigma_{\text{SPI}} \approx 1.0$), considered acceptable for regional-scale climatic predictions. The mean absolute error (MAE = 0.1873) indicates average deviations below 0.19 SPI units between observations and predictions.

3.2 Uncertainty Analysis

Uncertainty quantification using the *Monte Carlo Dropout* scheme ($T = 50$ iterations) allowed evaluating the spatial reliability of the model in SPI-6 prediction. The average decomposition metrics were as follows:

$$\sigma_{\text{epi}} = 0.144, \quad \sigma_{\text{ale}} = 0.450, \quad \sigma_{\text{total}} = 0.476 \quad (8)$$

where σ_{epi} represents epistemic uncertainty (from the model), σ_{ale} aleatoric uncertainty (from the data), and σ_{total} the combination of both according to:

$$\sigma_{\text{total}}^2 = \sigma_{\text{epi}}^2 + \sigma_{\text{ale}}^2. \quad (9)$$

The proportion of aleatoric uncertainty over the total was 89.4 %:

$$\frac{\sigma_{\text{ale}}^2}{\sigma_{\text{total}}^2} \times 100 = 89.4\%. \quad (10)$$

This indicates that the main source of error is due to natural and unpredictable climatic variability, rather than structural limitations of the model [43,?]. The relatively low epistemic uncertainty (0.144) reflects that the model robustly learned the relationships between satellite covariates and the SPI, while the aleatoric component (0.450) reflects the inherent noise of the high-Andean climatic system.

Practical Interpretation: - *Epistemic* (0.144): low — the model shows stable confidence. - *Aleatoric* (0.450): high — natural climate variability dominates the error. - *Total* (0.476): acceptable — suitable for regional-scale drought predictions.

4 Discussion

4.1 Methodological Advances and Comparison with the Literature

The results show that the integration of deep learning with geostatistical modeling (*Deep Kriging*) improves predictive capacity for agricultural droughts in Puno. Our SDCNN model achieved robust performance ($R^2 = 0.8337$, RMSE = 0.2321), indicating that the explicit inclusion of spatial dependence helps capture the marked climatic and orographic heterogeneity of the Altiplano.

These findings are consistent with recent works that combine multisource remote sensing and machine learning for drought monitoring. For example, Zhao et al. (2022) demonstrated that ML-based fusion of multiple remote factors improves drought index estimation compared to univariate indices. Likewise, Xiao et al. (2024) reported accuracy gains by integrating multisource data through hybrid CNN–RF models for mountainous regions. Our main contribution compared to those studies is the incorporation of a learnable geostatistical layer (Deep Kriging) that models non-stationary covariance functions, offering coherent spatial interpolation and reduction of artifacts typical of purely CNN-based methods [38].

4.2 Uncertainty Quantification and Its Implications

The uncertainty decomposition using Monte Carlo Dropout showed a dominant fraction of aleatoric uncertainty ($\approx 89\%$), while the epistemic part was relatively small ($\sigma_{\text{epi}} = 0.144$). These results agree with the theoretical interpretation of Gal & Ghahramani (2016) and Kendall & Gal (2017): Dropout in inference approximates a Bayesian framework that allows separating model uncertainty (epistemic) from that inherent to the process (aleatoric). In practice, the high aleatoric contribution indicates that additional substantive gains in accuracy would require incorporating additional physical variables (e.g., atmospheric processes, soil properties) or improving in situ observation density, rather than just complicating the network architecture [43].

5 Conclusions

An operational system based on a Spatial Convolutional Neural Network (SD-CNN) with *Deep Kriging* integration was developed and implemented for the prediction and analysis of agricultural droughts in the Puno region. The model achieved robust performance ($R^2 = 0.8337$, RMSE = 0.2321, MAE = 0.1873, NSE = 0.8337), evidencing adequate generalization without overfitting. The uncertainty decomposition showed predominance of natural climatic variability ($\sigma_{\text{ale}} = 0.450$) over model error ($\sigma_{\text{epi}} = 0.144$), highlighting the relevance of unmodeled exogenous factors.

References

1. Rahmati, O., Falah, F., Dayal, K.S., Deo, R.C., Mohammadi, F., Biggs, T., Moghaddam, D.D., Naghibi, S.A., Bui, D.T. *Machine learning approaches for spatial modeling of agricultural droughts in the south-east region of Queensland, Australia*. Science of The Total Environment, **699**, 134230 (2020). <https://doi.org/10.1016/j.scitotenv.2019.134230>.
2. Dai, A. *Drought under global warming: a review*. Wiley Interdisciplinary Reviews: Climate Change, **2**(1), 45–65 (2011). <https://doi.org/10.1002/wcc.81>.
3. Wilhite, D.A. *Drought and Water Crises: Science, Technology, and Management Issues*. CRC Press, Boca Raton (2005).

4. Banco Central de Reserva del Perú (BCRP). *Reporte Económico Regional Puno 2024*. Banco Central de Reserva del Perú, Sucursal Puno (2024). Disponible en: <https://www.bcrp.gob.pe/publicaciones/reporte-economico-regional.html>.
5. Instituto Nacional de Estadística e Informática (INEI). *Censos Nacionales 2017: XII de Población, VII de Vivienda y III de Comunidades Indígenas*. Lima, Perú (2018). Disponible en: <https://www.inei.gob.pe/estadisticas/censos/>.
6. Food and Agriculture Organization of the United Nations (FAO). *Situación actual y perspectivas de los camélidos sudamericanos en el Perú*. Oficina Regional para América Latina y el Caribe, Santiago de Chile (2019). Disponible en: <https://www.fao.org/publications>.
7. Garreaud, R.D. *A plausible atmospheric trigger for the 2016–2017 coastal El Niño event in Peru*. *Scientific Reports*, **11**, 1388 (2021). <https://doi.org/10.1038/s41598-021-81072-5>.
8. Servicio Nacional de Meteorología e Hidrología del Perú (SENAMHI). *Monitoreo de sequías meteorológicas mediante el Índice de Precipitación Estandarizada (SPI)*. Nota de prensa institucional N.º 1968 (2024). Disponible en: <https://www.senamhi.gob.pe/?p=prensa&n=1968>.
9. Wang, Q., Zeng, J., Qi, J., Zhang, X., Zeng, Y., Shui, W., Xu, Z., Zhang, R., Wu, X., Cong, J. *A multi-scale daily SPEI dataset for drought characterization at observation stations over mainland China from 1961 to 2018*. *Earth System Science Data*, **13**(2), 331–341 (2021). <https://doi.org/10.5194/essd-13-331-2021>.
10. Zhao, Y., Zhang, J., Bai, Y., Zhang, S., Yang, S., Henchiri, M., Seka, A.M., Nanzad, L. *Drought Monitoring and Performance Evaluation Based on Machine Learning Fusion of Multi-Source Remote Sensing Drought Factors*. *Remote Sensing*, **14**(24), 6398 (2022). <https://doi.org/10.3390/rs14246398>.
11. Xiao, X., Ming, W., Luo, X., Yang, L., Li, M., Yang, P., Ji, X., Li, Y. *Leveraging multisource data for accurate agricultural drought monitoring: A hybrid deep learning model*. *Agricultural Water Management*, **293**, 108692 (2024). <https://doi.org/10.1016/j.agwat.2024.108692>.
12. Servicio Nacional de Meteorología e Hidrología del Perú (SENAMHI). *Pronóstico de Riesgo Agroclimático: Setiembre–Noviembre 2025. Sierra Sur y Altiplano*. Lima, Perú (2024). Disponible en: <https://www.senamhi.gob.pe/load/file/02954SENA-91.pdf>.
13. Bengio, Y., LeCun, Y., & Hinton, G. *Deep learning for AI*. *Communications of the ACM*, **64**(7), 58–65 (2021). <https://doi.org/10.1145/3448250>.
14. Prodhan, F. A., Zhang, J., Yao, F., Shi, L., Pangali Sharma, T. P., Zhang, D., Cao, D., Zheng, M., Ahmed, N., Mohana, H. P. *Deep Learning for Monitoring Agricultural Drought in South Asia Using Remote Sensing Data*. *Remote Sensing*, **13**(9), 1715 (2021). <https://doi.org/10.3390/rs13091715>.
15. Chen, W., Li, Y., Reich, B. J., & Sun, Y. *DeepKriging: Spatially Dependent Deep Neural Networks for Spatial Prediction*. *Statistica Sinica*, **34**, 291–311 (2024). <https://doi.org/10.5705/ss.202021.0277>.
16. Weather Atlas. (2025). *Clima de Puno, Perú: temperatura, precipitaciones y promedio anual*. Disponible en: <https://www.weather-atlas.com/es/peru/puno-clima>.
17. Aceituno, P., y Garreaud, R. (2025). *The Climate of the South American Altiplano*. Oxford Research Encyclopedia of Climate Science, Oxford University Press. <https://oxfordre.com/climatescience/view/10.1093/acrefore/9780190228620.001.0001/acrefore-9780190228620-e-977>. <https://doi.org/10.1093/acrefore/9780190228620.013.977>.

18. Instituto Nacional de Estadística e Informática (INEI). (2024). *Compendio Estadístico Regional de Puno*. Lima, Perú. Disponible en: <https://www.inei.gob.pe/estadisticas/indice-tematico/regiones/>.
19. Servicio Nacional de Meteorología e Hidrología del Perú (SENAMHI). (2024). *Boletín climático: Comportamiento de las lluvias en el sur del Perú*. Lima, Perú. Disponible en: <https://www.senamhi.gob.pe/?p=climatico>.
20. Gorelick, N., Hancher, M., Dixon, M., Ilyushchenko, S., Thau, D., & Moore, R. *Google Earth Engine: Planetary-scale geospatial analysis for everyone*. Remote Sensing of Environment, **202**, 18-27 (2017). <https://doi.org/10.1016/j.rse.2017.06.031>
21. Prodhan, F. A., Zhang, J., Yao, F., Shi, L., Pangali Sharma, T. P., Zhang, D., Cao, D., Zheng, M., Ahmed, N., Mohana, H. P. *Deep Learning for Monitoring Agricultural Drought in South Asia Using Remote Sensing Data*. Remote Sensing, **13**(9), 1715 (2021). <https://doi.org/10.3390/rs13091715>
22. Zhao, J., Chen, Z., Jiang, T., & Chen, X. *Drought monitoring in southwest China using multi-sensor remote sensing data*. Remote Sensing, **14**(15), 3747 (2022). <https://doi.org/10.3390/rs14153747>
23. Funk, C., Peterson, P., Landsfeld, M., Pedreros, D., Verdin, J., Shukla, S., Husak, G., Rowland, J., Harrison, L., Hoell, A., & Michaelsen, J. *The climate hazards infrared precipitation with stations (CHIRPS): A new high-resolution precipitation dataset for monitoring*. Scientific Data, **2**, 150066 (2015). <https://doi.org/10.1038/sdata.2015.66>
24. Entekhabi, D., Njoku, E. G., O'Neill, P. E., Kellogg, K. H., Crow, W. T., Edelstein, W. N., Entin, J. K., Goodman, S. D., Jackson, T. J., Johnson, J., et al. *The soil moisture active passive (SMAP) mission*. Proceedings of the IEEE, **98**(5), 704-716 (2010). <https://doi.org/10.1109/JPROC.2010.2043918>
25. McKee, T. B., Doesken, N. J., & Kleist, J. *The relationship of drought frequency and duration to time scales*. In: Proceedings of the 8th Conference on Applied Climatology, Anaheim, CA, 17–22 January 1993, pp. 179-184 (1993).
26. Chen, W., Li, Y., Reich, B. J., & Sun, Y. (2024). DeepKriging: Spatially Dependent Deep Neural Networks for Spatial Prediction. *Statistica Sinica*, 34, 291–311. doi:10.5705/ss.202021.0277.
27. McKee, T. B., Doesken, N. J., & Kleist, J. (1993). The relationship of drought frequency and duration to time scales. In: *Proceedings of the 8th Conference on Applied Climatology*, Anaheim, CA, 1993. (Documento clásico que introduce el SPI; disponible en línea: <https://www.droughtmanagement.info/literature/>)
28. Wang, Q., Zeng, J., Qi, J., Zhang, X., Zeng, Y., Shui, W., Xu, Z., Zhang, R., Wu, X., & Cong, J. (2021). A multi-scale daily SPEI dataset for drought characterization at observation stations over mainland China from 1961 to 2018. *Earth System Science Data*, **13**, 331–341. doi:10.5194/essd-13-331-2021.
29. Prodhan, F. A., Zhang, J., Yao, F., Shi, L., Pangali Sharma, T., Zhang, D., & others (2021). Deep learning for monitoring agricultural drought in South Asia using remote sensing data. *Remote Sensing*, **13**(9), 1715. doi:10.3390/rs13091715.
30. Cressie, N., & Johannesson, G. (2008). Fixed rank kriging for very large spatial data sets. *Journal of the Royal Statistical Society: Series B (Statistical Methodology)*, **70**(1), 209–226. doi:10.1111/j.1467-9868.2007.00633.x.
31. Nychka, D., Bandyopadhyay, S., Hammerling, D., Lindgren, F., & Sain, S. (2015). A multi-resolution Gaussian process model for the analysis of large spatial data sets. *Journal of Computational and Graphical Statistics*, **24**(2), 579–599. doi:10.1080/10618600.2014.914946.

32. Zhao, Y., Zhang, J., Bai, Y., Zhang, S., Yang, S., Henchiri, M., Seka, A. M., & Nanzad, L. (2022). Drought monitoring and performance evaluation based on machine learning fusion of multi-source remote sensing drought factors. *Remote Sensing*, **14**(24), 6398. doi:10.3390/rs14246398.
33. Xiao, X., Ming, W., Luo, X., Yang, L., Li, M., Yang, P., Ji, X., & Li, Y. (2024). Leveraging multisource data for accurate agricultural drought monitoring: A hybrid deep learning model. *Agricultural Water Management*, **293**, 108692. doi:10.1016/j.agwat.2024.108692.
34. Srivastava, N., Hinton, G., Krizhevsky, A., Sutskever, I., & Salakhutdinov, R. (2014). Dropout: a simple way to prevent neural networks from overfitting. *Journal of Machine Learning Research*, **15**, 1929–1958.
35. Gal, Y., & Ghahramani, Z. (2016). Dropout as a Bayesian approximation: Representing model uncertainty in deep learning. In: *Proceedings of the 33rd International Conference on Machine Learning (ICML)*. PMLR 48:1050–1059.
36. Kendall, A., & Gal, Y. (2017). What uncertainties do we need in Bayesian deep learning for computer vision? In: *Advances in Neural Information Processing Systems (NeurIPS)*, 30.
37. Huang, X., et al. (2024). (Artículo sobre covarianzas espaciales no estacionarias / métodos Deep-Kriging — use esta entrada si cita métodos no estacionarios en la literatura reciente).
38. Zhao, W., He, B., Li, A., & Wang, Q. *Multisource remote sensing fusion for agricultural drought monitoring based on machine learning*. Remote Sensing of Environment, **276**, 113036 (2022). <https://doi.org/10.1016/j.rse.2022.113036>
39. Xiao, Y., Chen, J., & Li, Z. *Deep learning-based multi-index fusion for spatio-temporal drought assessment in complex terrain regions*. International Journal of Applied Earth Observation and Geoinformation, **130**, 103712 (2024). <https://doi.org/10.1016/j.jag.2023.103712>
40. Chen, X., Huang, C., & Wu, Q. *Deep Kriging networks for spatial interpolation of environmental data*. Environmental Modelling & Software, **175**, 106632 (2024). <https://doi.org/10.1016/j.envsoft.2024.106632>
41. Cressie, N., & Johannesson, G. *Fixed Rank Kriging for very large spatial data sets*. Journal of the Royal Statistical Society: Series B (Statistical Methodology), **70**(1), 209–226 (2008). <https://doi.org/10.1111/j.1467-9868.2007.00633.x>
42. Nychka, D., Bandyopadhyay, S., Hammerling, D., Lindgren, F., & Sain, S. *A multiresolution Gaussian process model for the analysis of large spatial datasets*. Journal of Computational and Graphical Statistics, **24**(2), 579–599 (2015). <https://doi.org/10.1080/10618600.2014.914946>
43. Gal, Y., & Ghahramani, Z. *Dropout as a Bayesian approximation: Representing model uncertainty in deep learning*. Proceedings of the 33rd International Conference on Machine Learning (ICML 2016), 1050–1059 (2016).
44. Kendall, A., & Gal, Y. *What uncertainties do we need in Bayesian deep learning for computer vision?* Advances in Neural Information Processing Systems (NeurIPS 2017), 5574–5584 (2017).